



# Acoustics 2008

Geelong, Victoria, Australia 24 to 26 November 2008

## Acoustics and Sustainability:

How should acoustics adapt to meet future demands?

### On modelling the seabed in order to predict low-frequency acoustic Transmission Loss in shallow water

Marshall V. Hall

9 Moya Crescent, Kingsgrove NSW, Australia

#### ABSTRACT

To compute Transmission Loss (TL) in shallow water, the required environmental parameters include a geoacoustic model (GAM) of the seabed, the sound-speed profile of the water layer, and roughness of the sea-surface and sea-floor. The GAM is estimated with regression equations from geological properties, which are held in a geographic database. TL can be affected by the GAM down to a few wavelengths below the sea-floor, but such data is sparse. In practice, sonar prediction systems assume that the seabed is uniform from the sea-floor down. A question that arises is the degree to which computed low-frequency TL can consequently differ from actual TL. This issue is addressed by examining the results of a TL experiment that was accompanied by measurements of sea-floor and seawater properties. At 100 Hz the computed TL compared well with the data, whereas at 50 Hz the computed TL was too high (by 18 dB at 20-km range). This error can be attributed to the existence of a reflecting basement within the seabed that was not accounted for. When such acoustic effects are found, seabed databases should be modified to include an appropriate basement.

#### INTRODUCTION

The aim of this paper is to present an example of the possible errors in predictions of low-frequency Transmission Loss (TL) that are based on the sediment type at the sea-floor, and thus neglect the variation in sediment type that can occur beneath the sea-floor. A TL measurement that was accompanied by measurements of appropriate sea-floor and water column properties is examined. TL is computed with the usual assumptions:

- the geoacoustic properties at the sea-floor are obtained via standard regressions from the sediment mean grain size, and
- a geoacoustic model (GAM) of the seabed is derived, based on the assumption that the mean grain size is independent of depth and held constant at its sea-floor value.

The computed TL is then compared with the measured value, and possible explanations for the difference are canvassed. The TL algorithm selected for the calculations is RAM (Collins, 1993), on the basis of considerations that will be described later in the paper.

#### OUTLINE OF TRANSMISSION LOSS DATA

Ideally, a propagation run designed to investigate sensitivity to seabed characterisation would be in shallow water and have a porous sea-floor, so as to maximise the importance of the sub-bottom. In order to minimise errors in computing TL for the run, the surface and sea-floor roughness should be negligible, and the environment range-independent. If a range-independent run is unavailable, then it is necessary that the range dependence can be modelled. In examining the available data from TL runs conducted on the Australian continental shelf, all runs exhibited range-dependence to some degree. The run that has been selected, which will be

referred to as "Run F", was conducted by the Australian Navy ship HMAS COOK, with data being recorded by DSTO staff. This run is one of a group that has been referred to by Jones et al (2006). The sea-floor was silt with an average depth of 56 m. The surface and sea-floor roughness were both small (and approximately constant along the line), and the properties of the water-layer and sea-floor were measured at the start and end of the propagation line. The sound receiver was a calibrated sonobuoy hydrophone. The sound sources were small explosive charges fired at ranges from 3.5 to 30 km. The shot data were analysed at frequencies in third-octave steps (and with third-octave bandwidths) from around 20 Hz to 4 kHz.

#### CHOICE OF FREQUENCY FOR COMPARISON

The reasons for choosing a low frequency are as follows:

(a) Due to nonlinear effects changing the shape of the shock wave, the Source Level of explosive charges varies with range in general, but the variation over 30 km is negligible at frequencies less than around 300 Hz.

(b) The acoustic effect of boundary roughness increases with the ratio of RMS roughness to acoustic wavelength, and can be computed by particular TL algorithms. The writer has found that providing this ratio is less than one, the effect can be obtained using OAST (Schmidt, 1999). Since the greatest roughness encountered in Run F has an RMS value of 0.8 m (the sea-floor), this condition is met at frequencies less than around 2 kHz.

(c) In cases where a surface mixed layer is present, the seabed will play a minor role at frequencies above the cut-off frequency of the resulting sonic duct. For the purposes of this paper it is better for the frequency to be below the cut-off

frequency. On Run F the thickness of the sonic duct was 45 m at the Start of the Line (SOL) and decreased as the run progressed. For a 45-m duct the corresponding cut-off frequency is 600 Hz. For frequencies no more than around 100 Hz, the variation in duct thickness that did occur will not have a significant effect on TL. Nevertheless, the range-varying profiles will be taken into account when TL is computed.

On the other hand, there is a limit to how low a suitable frequency can be, for the following reasons.

(d) As frequency decreases below 50 Hz, it becomes more difficult to obtain consistency in Source Level measurements (due to the surface reflection), with the result that there is uncertainty in shot Source Level.

(e) The relevance of the results (to the detection of underwater vehicles) generally decreases as frequency decreases below 50 Hz.

(f) The number of available data decreases as frequency goes below 50 Hz, due to the combined effects of low-frequency cut-off and increasing background noise.

With regard to the aims of the present study, it has been sufficient to examine the data at frequencies of 50 and 100 Hz.

## SEA SURFACE ROUGHNESS

During Run F the wind-speed was reported as 2 knot (1 m/s). The wind-wave significant height ( $H_s$ ) was estimated from wind-speed using Pierson's (1964) expression:

$$H_s = 0.0214 U^2,$$

where  $H_s$  is in metres and  $U$  is wind-speed (m/s) measured at the standard anemometer height of 19.5 m (if measured at a different height, the wind-speed should first be amended to its estimated value at 19.5 m). For the reported wind speed, the corresponding significant wind-wave height was 0.02 m.

The swell heights as reported by Navy observers are assumed to be the "significant wave height" of the swell. Since the reported swell height was 0 m (to the nearest quarter-metre), the total significant wave height of both wind-waves and swell was no more than 0.1 m. TL algorithms that include the effect of roughness require a value for the RMS roughness, which is 25% of the significant wave height (American Meteorological Society, 2000). The RMS roughness was thus no more than 0.025 m.

A TL algorithm that caters for (range-independent) roughness is OAST, although it does not cater for range-dependence in other properties. The RAM algorithm caters for range dependence in other properties, but not for surface roughness. The possible significance of surface roughness was estimated by defining the sound-speed profile and GAM for both the SOL and EOL, and applying these to OAST both with and without surface roughness. It was found that the above surface roughness has negligible effect on TL at frequencies of 50 or 100 Hz.

## SOUND-SPEED PROFILES

Two temperature profiles were measured during Run F, one at SOL and the other at the End of the Line (EOL), 30 km distant. These profiles are shown in **Figure 1**. Since these profiles differ by no more than 1 °C at any depth, it is reasonable to assume, for the purpose of computing TL, that the temperature at any depth varied linearly with range

The sound-speed profiles were computed using Mackenzie's (1981) formula. A value for salinity for the appropriate location and season was obtained from World Ocean Atlas (2005).

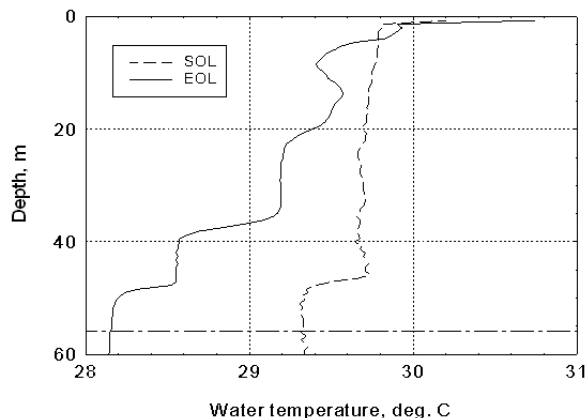


**Figure 1:** Measured water temperature profiles at the SOL and EOL of Run F.

In characterising the range-dependence of sound-speed profile along Run F for RAM, it is necessary that the propagation line be divided into a number of segments, over each of which the environment must be range-independent. Given that the changes in water layer profile are not large, the following simple procedure was followed:

- The SOL and EOL sound-speed profiles were examined, and it was concluded that a common depth resolution of 5 m would suffice for computing TL at low frequencies
- The SOL and EOL sound-speeds at the 11 depths from 0 to 50 m, and 56 m, were noted
- The 30-km line was divided into six (5-km) segments
- The sound-speeds at the 12 depths, along each segment, were set to their linearly-interpolated values at the segment's midpoint.

The six sound speed profiles that resulted are shown in **Figure 2**.

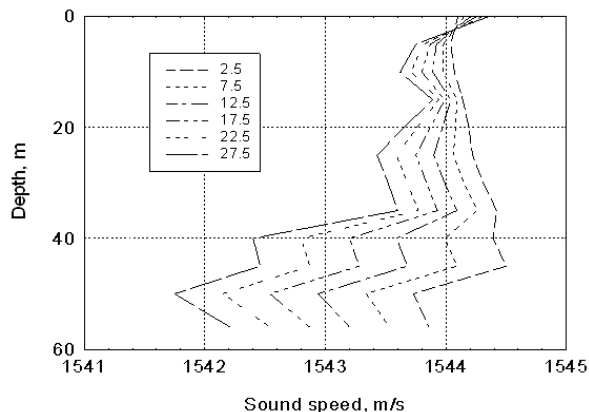


**Figure 2:** Sound-speed profiles for the six segments of Run F, based on the hypothesised linear range dependence in water temperature.

## BATHYMETRY

The ship's high-frequency Echo Sounder was operated along the propagation line, although there are gaps in the data. The bathymetry was recorded digitally at 750 points out to 15-km range, and recorded manually at a further 10 points between 15 and 30 km. The linear regression line through the data for seafloor depth (SFD) is:

$$\text{SFD}(r) = 56.8 - 0.073 r,$$

where  $r$  is the range from SOL in km. Thus SFD changes from 56.8 m at SOL to 54.6 m at EOL, a decrease of 2.2 m in 30 km.

The RMS of the residuals relative to the regression curve is 0.8 m. In operating RAM, this roughness as such cannot be used; instead, the 760 individual seafloor depths were listed in the bathymetry section of the RAM input file.

**GEOLOGY**

The proportion of calcareous material in the grab samples from the SOL and EOL of Run F are reported to be between 85% and 90%. The mean grain size (MGS) of these two grab samples are  $4.8 \phi$  and  $6.9 \phi$  respectively. In view of other information on the seafloor in the area, it can be assumed that MGS varies monotonically with range along the line.

RAM requires that the seabed GAM be provided as uniform along each of a number of segments. Since the difference in MGS from SOL to EOL is not large, it has been assumed that MGS varies linearly with range. The 30-km line has again been divided into six segments, and the MGS for each segment has been set to its horizontally-interpolated value at the segment's midpoint. The uncertainty in TL due to various ways in which MGS could vary with range has been neglected since, for the purpose of this study, the important feature is the comparison between two frequencies, and the range-dependence of MGS will of course be the same for both. The results are illustrated in **Figure 3**.

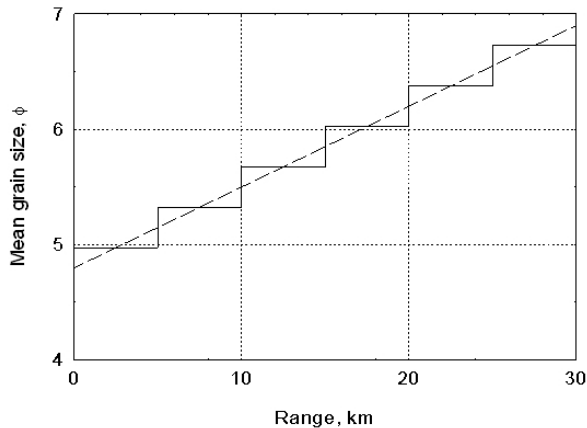


**Figure 3:** Mean Grain Size from SOL to EOL, and for the six segments. KEY: dashed line – hypothesised linear-range dependence; solid line – range-dependence supplied to RAM.

**GEOACOUSTIC MODEL**

The seabed acoustic parameters that comprise a GAM are: density ( $D_y$ ), sound speed ( $C_p$ ), shear speed ( $C_s$ ), sound attenuation coefficient ( $A_p$ ), and shear attenuation coefficient ( $A_s$ ). These are individually estimated from MGS using published regressions. (Although this method is subject to error due to spread of data around the regression curve, Sonar Prediction Systems use the same method).

**Density**

Since silt at the seafloor has an average porosity of 60% (Richardson & Briggs, 1993), it becomes more compact as its confining pressure increases, and its density increases with depth below the seafloor. Data for the density gradient in continental shelf silt are not to hand. For deep-sea calcareous sediments, Hamilton (1976) reported an increase in density of 0.17 g/cc from the seafloor to a depth of 100 m.

A regression for MGS in terms of seafloor density was presented by Richardson & Briggs (1993):

$$MGS = 22.85 - 10.275 D_y, \tag{1}$$

and this has been inverted to compute  $D_y$  (in g/cc) for a given MGS, notwithstanding that this regression was not designed for that purpose. (From a graph of data in that paper, the possible error in  $D_y$  for a given MGS is approximately  $\pm 0.2$  g/cc). The resulting values of seafloor density at SOL, EOL, and the six segment midpoints are shown in **Figure 4** (the curve shown is the linear interpolation). Also shown are the densities at 100 m below the seafloor. For each range-segment, RAM was supplied with a density profile over the depth interval from the seafloor to 100 m below the seafloor. The values supplied for these depths of 0 and 100 m are indicated by the points (other than SOL and EOL) in **Figure 4**.

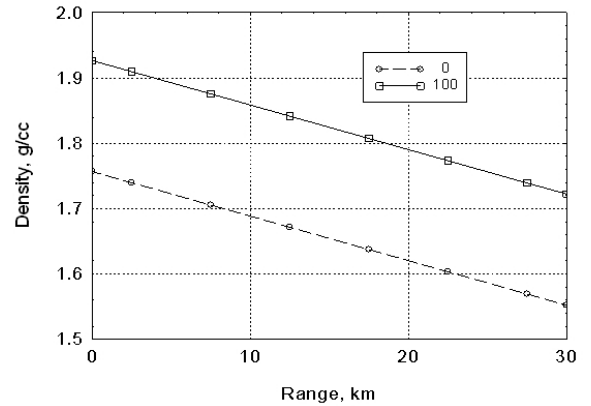


**Figure 4:** Estimated seabed densities at SOL and EOL, and for the six segments. Numerals in the legend denote depth below seafloor (m). The range-dependence supplied to RAM was a sequence of six steps.

**Porosity**

Porosity ( $\beta$ ) and density are related through the following expression:

$$D_y = \beta D_w + (1 - \beta) D_g$$

where  $D_w$  is the density of the water, and  $D_g$  is the density of the solid.

If  $D_w$  and  $D_g$  are set to appropriate values (1.022 and 2.7 g/cc) then porosity can be obtained from density. The results for both the seafloor and 100 m below the seafloor are shown in **Figure 5**. At the seafloor, the estimated porosity ranges from 0.56 to 0.68, while at a depth of 100 m it ranges from 0.46 to 0.58.

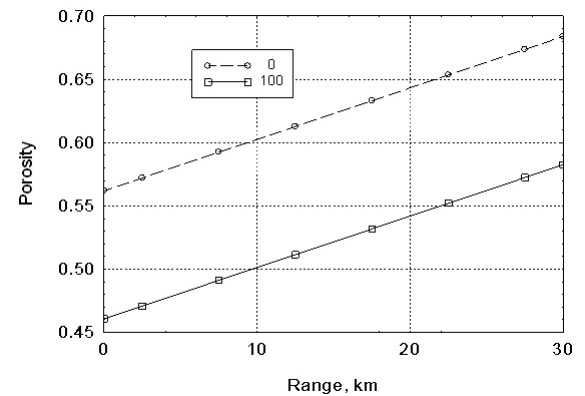


**Figure 5:** Estimated seabed porosities at the SOL, EOL, and the mid points of the six range-segments. Numerals in the legend denote depth below the seafloor (m).

**Shear speed.**

Shear speed in unconsolidated sediment is due to confining pressure. It is thus zero at the seafloor, and increases with depth below the seafloor. An empirical expression for the  $C_s$  profile in silt has been presented by Ohta and Goto (1978):

$$C_s(z) = 79 z^{0.312} \tag{2}$$

where  $z$  is depth (m) below the seafloor. In this profile,  $C_s$  increases from 79 to 332 m/s as depth increases from 1 to 100 m.

**Sound speed.**

In unconsolidated sediment, sound speed increases with confining pressure and decreases with porosity', and therefore increases with depth below the seafloor. The regression obtained by Hamilton (1985) for continental-terrace silt-clays can be expressed as:

$$C_p(z) = C_p(0) + 0.71 z \tag{3}$$

where  $C_p(z)$  is the sound speed at depth  $z$  below the seafloor.

Sound speed at the seafloor is characterised by its ratio to the bottom seawater sound speed ( $C_w$ ). A regression for this ratio as a function of MGS has been reported by Richardson and Briggs (2004). Values for  $C_p(0)$  obtained from this regression, as applied to the MGS curve in **Figure 3**, are shown in **Figure 6** (the curve shown is the interpolation between the values obtained at each MGS). Also shown are the corresponding values 100 m below the seafloor, obtained using Eq. (3).

On operating OAST on the SOL environment, with  $C_p$  increasing in steps consistent with Eq. (3) to a depth of 100 m, it was found that inclusion of the  $C_s$  profile as per Eq. (2) yielded approximately the same TL as did setting  $C_s = 0$ . For Run F it is therefore satisfactory to set  $C_p$  in accordance with Eq. (3), and to neglect  $C_s$ . In view of this finding, RAM can be used on Run F with negligible error. For each range-segment, RAM was supplied with a sound-speed profile from the seafloor to 100 m below the seafloor.

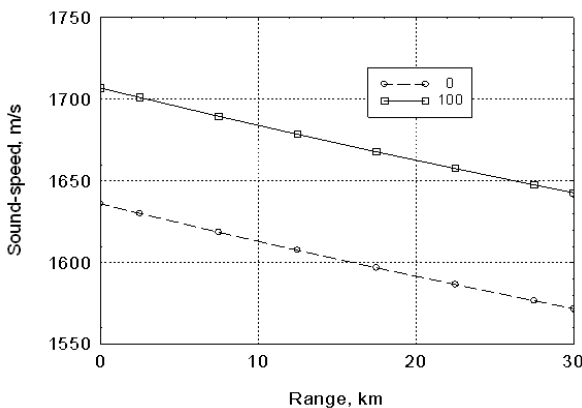


**Figure 6:** Estimated seabed sound speeds at SOL and EOL, and for the six segments. Numerals in the legend denote depth below seafloor (m). The range-dependence supplied to RAM was a sequence of six steps.

**Sound attenuation**

In unconsolidated sediment, sound attenuation is affected mainly by porosity, and therefore varies with depth below the seafloor. As a function of porosity, attenuation has a maximum at around 0.52 (Hamilton, 1972). If the seafloor porosity exceeds 0.52, as it generally will for silt (as per **Figure 5**), then with increasing depth below the seafloor, porosity will decrease and attenuation will increase. As a function of depth, porosity is obtained from density, and attenuation is

obtained from Hamilton's (1972) regression for attenuation in terms of porosity. The coefficient reported by Hamilton ( $K_p$ ) was attenuation per unit frequency (Hz) per unit distance (km). RAM requires however that the coefficient be attenuation over a distance of one wavelength within the seabed ( $A_p$ ). The relation between these two coefficients is:

$$A_p = K_p * C_p / 1000.$$

For each range-segment, RAM was supplied with a profile of  $A_p$  from the seafloor to 100 m below the seafloor. The values supplied for the seafloor were the values indicated by the six points (other than SOL and EOL) in **Figure 7** (the curve shown is the interpolation between the values obtained for the mid-point of each segment). Also shown are the corresponding values 100 m below the seafloor, obtained using the lower porosities at that depth. It can be seen from **Figure 5** that the attenuation peak (porosity 0.52) occurs at 100-m depth at a range of 14.5 km; and the effect of this is evident for the corresponding curve in **Figure 7**.

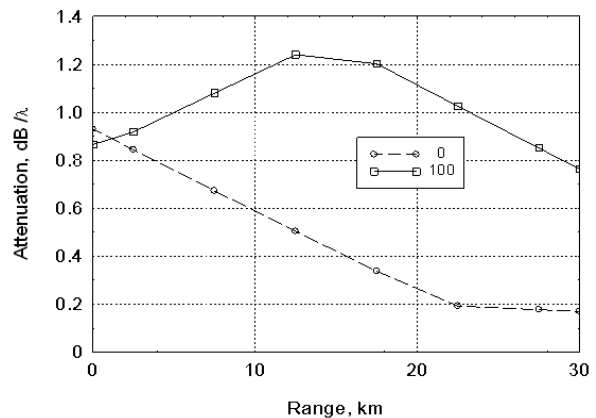


**Figure 7:** Seabed sound attenuation coefficients at SOL and EOL, and for the six segments. Numerals in the legend denote depth below seafloor (m). The range-dependence supplied to RAM was a sequence of six steps.

**COMPARISON OF COMPUTED WITH MEASURED TL**

The measured and computed TL at frequency 100 Hz are shown in **Figure 8**. The computed curve shows an interference pattern at ranges up to around 12 km since it applies to a single frequency, whereas the data apply to a third-octave bandwidth. It can be seen that the computed TL is somewhat higher than the data; the difference is 5 dB at 20-km range, and increases to 7 dB at the maximum range of 30 km. The computed curve is fairly robust, since when it was repeated with a GAM that was constant with depth, the result obtained was quite similar. One would conclude from it that either the silt seafloor was a better reflector than modelled (had a lower porosity), or that there was a low-porosity sub-bottom basement.

When the results at 50 Hz are examined however (Figure 9), the discrepancy between experiment and theory is large. The computed TL is significantly higher than the data; the difference is 18 dB at 20 km, and appears that it would approach 30 dB if extrapolated to 30 km. This large difference cannot be attributed to an error in the modelling of the silt. The only explanation is that there is a sub-bottom low-porosity basement. The basement would be a few metres deep, where it would have a large effect on 50-Hz sound, but a small effect on 100-Hz sound.

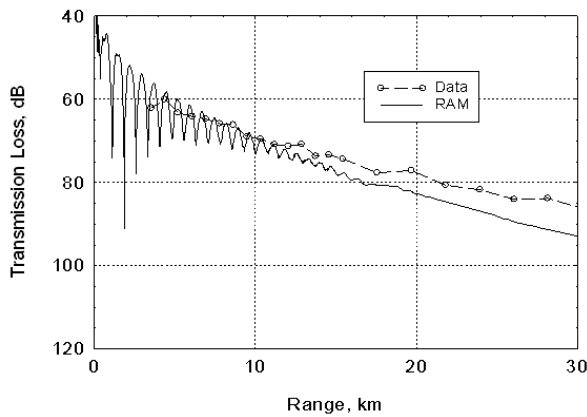


**Figure 8:** Measured and computed TL along Run F at frequency 100 Hz.

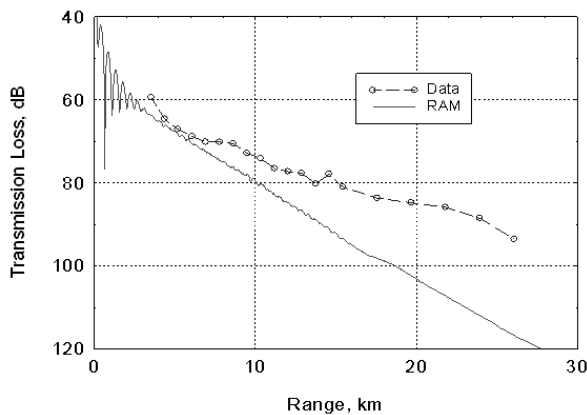


**Figure 9:** Measured and computed TL along run F at frequency 50 Hz.

**CONCLUSIONS**

By examining a suitable measurement of transmission loss, it has been found that even careful modelling at 50 Hz fails to yield a calculated TL that is at all useful, if it is assumed that the seabed is a half-space of homogenous silt. The only explanation for the measured TL is the presence of a sub-bottom low-porosity basement. If a Sonar Prediction System is applied to Run F, it will produce a similar error, since there is no relevant sub-bottom geological information available. It is therefore important that stakeholders in such systems search for features similar to those of Run F, measure TL at low frequencies, and adjust their seabed database so that their prediction system will produce realistic results.

**ACKNOWLEDGMENT**

The data reported here is the property of the DSTO.

**REFERENCES**

American Meteorological Society 2000, <http://amsglossary.allenpress.com/glossary/search?p=1&query=significant+wave+height&submit=Search>

Collins, M. D. 1993, "A split-step Pade solution for the parabolic equation method", *Journal of the Acoustical Society of America*, vol. 93, pp 1736-1742. A user's guide and updates of the code are available via anonymous ftp from ram.nrl.navy.mil

Hamilton, E. L. 1972, "Compressional wave attenuation in marine sediments", *Geophysics*, vol. 37, pp 620-645.

Hamilton, E. L. 1976, "Variations of density and porosity with depth in deep-sea sediments", *Journal of Sedimentary Petrology*, vol. 46, pp 280-300.

Hamilton, E. L. 1985, "Sound velocity as a function of depth in marine sediments", *Journal of the Acoustical Society of America*, vol. 78, pp 1348-1355.

Jones, A.D., Maggi, A.L., Clarke, P.A., and Duncan A.J. 2006, "Analysis and Simulation of an Extended Data Set of Waveforms Received from Small Explosions in Shallow Oceans", *Proceedings of ACOUSTICS 2006*, Christchurch, New Zealand, pp. 481-488.

Mackenzie K. V. 1981, "Nine-term equation for sound speed in the oceans", *Journal of the Acoustical Society of America*, vol. 70, pp 807-812.

Ohta, Y. and Goto, N. 1978, "Empirical shear wave velocity equations in terms of characteristic soil indexes", *Earthquake Engineering & Structural Dynamics*, vol. 6, p. 167.

Pierson, W. J. 1964, "The Interpretation of Wave Spectrums in Terms of the Wind Profile instead of the Wind Measured at a Constant Height", *Journal of Geophysical Research*, vol. 69, pp 5191-5203.

Richardson, M. D. and Briggs, K. B. 1993, "On the use of acoustic impedance values to determine sediment properties", in 'Acoustic Classification and Mapping of the seabed', *Proceedings of the Institute of Acoustics*, vol. 15 (2), Bath UK, pp. 15-24.

Richardson, M. D. and Briggs, K. B. 2004, "Relationships among sediment physical and acoustic properties in siliciclastic and calcareous sediments", *Proceedings of the Seventh European Conference on Underwater Acoustics, ECUA 2004*, Delft, The Netherlands.

Schmidt, H. 1999, "OASES Ocean Acoustics and Seismic Exploration Synthesis (version 2.2)". Retrieved 1999, from <http://acoustics.mit.edu/faculty/henrik/oases.html>

World Ocean Atlas 2005, <http://www.nodc.noaa.gov/cgi-bin/OC5/WOA05/woa05.pl>